

MODELLING OF ELASTOPLASTIC DEFORMATION OF TRANSVERSELY ISOTROPIC ROTATING DISC OF VARIABLE DENSITY WITH SHAFT UNDER A RADIAL TEMPERATURE GRADIENT

MODELIRANJE ELASTOPLASTIČNE DEFORMACIJE TRANSVERZALNOG IZOTROPNOG ROTIRAJUĆEG DISKA PROMENLJIVE GUSTINE SA OSOVINOM POD UTICAJEM RADIJALNOG GRADIJENTA TEMPERATURE

Originalni naučni rad / Original scientific paper
UDK /UDC:

Rad primljen / Paper received: 7.12.2019

Adresa autora / Author's address:

¹) Depart. of Mathematics, Punjabi University, Patiala, India

²) Department of Mathematics, ICFAI University, Himachal Pradesh, India, email: pankaj_thakur15@yahoo.co.in

Keywords

- elastoplastic
- rotating disc
- transversely isotropic
- stresses
- strains, displacement
- temperature gradient

Abstract

This study deals with the elastoplastic deformation of transversely isotropic rotating disc of variable density with shaft subjected to temperature gradient by using transition theory of Seth and generalized strain measure theory. Solving the problems in classical plasticity theory needs the empirical assumption such as the yield criterion. This results from the use of direct strain measures that ignore the non-linear transition region where the yield occurs and the fact that plastic strains are never straight. The transition theory of Seth requires no ad-hoc assumptions such as yield condition, incompressibility condition, infinitesimal strains and creep strain laws. Therefore, generalized strain measure and transition theory are the general methods of solving a problem from which the classical theory assumptions can be obtained. The combined impacts of density, temperature, and angular speed have been displayed numerically and graphically. It is seen that the disc made of transversely isotropic material yields at the external surface of the disc, however, the disc of isotropic material yields at the internal surface of the disc as the density of the rotating disc increases from outer to inner surface with the increase of temperature and angular speed. The displacement of the isotropic rotating disc is higher than that of the transversely isotropic rotating disc.

INTRODUCTION

Rotating discs can be used in a variety of engineering applications such as flywheels, gas turbine engines, gears, compressors, computer disc drives, car disc brakes, shrink fits, circular saws, storage devices (hard disks, blue ray discs etc.). In these applications, the rotating disc is exposed to various loads and is additionally exposed to high temperatures. Under these conditions, the theoretical study of stress distribution and strain in a disc at high speed is of great practical use as the lifetime of machine parts can be enhanced

Ključne reči

- elastoplastičnost
- rotirajući disk
- transversalno izotropno
- naponi
- pomeranje i deformacije
- gradijent temperature

Izvod

U radu je primenom teorije prelaznih napona Seta i teorije mera generalisanih deformacija istražena elasto-plastična deformacija transversalnog izotropnog rotirajućeg diska, promenljive gustine, sa osovinom, koji je opterećen gradijentom temperature. Rešavanje problema u klasičnoj teoriji plastičnosti zahteva empirijsku pretpostavku kao što je kriterijum tečenja. Ovo je posledica primene direktnih mera deformacije, kojima se zanemaruje nelinearna prelazna oblast, u kojoj se javlja tečenje, kao i činjenice da plastične deformacije nisu pravolinijske. Teorija prelaznih napona Seta ne zahteva ad-hoc pretpostavke, kao što su kriterijum tečenja, uslov nestišljivosti, infinitezimalne deformacije i zakone puzanja. Stoga su generalisana mera deformacija i teorija prelaznih napona opšte metode za rešavanje problema, preko kojih se ostvaruju pretpostavke klasične teorije. Kombinovani uticaji gustine, temperature i ugaone brzine su predstavljeni numerički i grafički. Uočava se pojava tečenja na spoljnoj površini diska od transversalnog izotropnog materijala, međutim, kod diska od izotropnog materijala, tečenje se javlja na unutrašnjoj površini diska, pri povećanju gustine rotirajućeg diska u pravcu od spoljne ka unutrašnjoj površini, sa porastom temperature i ugaone brzine. Pomeranja kod izotropnog rotirajućeg diska su veća u odnosu na transversalni izotropni disk.

for a better understanding of the disc behaviour and an efficient rotational disc model for the task needed. The importance of rotating discs in engineering is significant in many problems and a long-standing field of study in the domain of mechanics of solids. The analytical elasticity-plasticity of such rotating disc of isotropic materials can be found in many books, /1-3, 5, 8, 18/. Laszlo /6/ began the theoretical treatment of rotating disc in 1925 and interests in this problem have never stopped. Researchers are dedicated to the study of rotating discs based on classical and

non-classical treatment to figure out the optimal design of structural components and not to confine themselves to the usual elastic regime, but to the elastoplastic regime due to the increasing material scarcity and higher material costs. In analysing the problem [4, 13-16] by classical treatment in elastoplastic (or elastic-plastic) structural components and creep deformation, researchers used assumptions: the deformation is small enough; incompressibility condition; yield criterion; etc. Starting from 1962, researchers used the transition theory of Seth [12] and generalised strain measure theory (non-classical treatment) which does not include any simplification of empirical assumptions such as the yield criterion. Many researches on the analysis of stresses and strains in rotating disc have been performed with regard to elastoplastic and creep transition in classical treatment. However, the studies using the non-classical treatment of this structural component are rather limited as compared to classical treatment even though the real behaviour of the transition of the material is nonlinear and the method neglects the empirical assumptions. In view of this, there is a need to investigate elastoplastic and creep transitional stresses and strains for different material symmetries of the disc having different parameters under different loading. Transition theory of Seth uses the generalized strain measure theory and asymptotic approach. The transition function through the combination of principal stresses at transition points of the differential system describing the deformed medium is successfully applied to a more general and wider range of problems. Pankaj [7] solved problems in elastic-plastic stresses of an isotropic rotating disc of infinitesimal deformation under steady state temperature.

The generalized principal strain measure is defined [12] as

$$e_{ii}^A = \int_0^{e_{ii}^A} (1 - 2e_{ii}^A)^{\frac{n}{2}-1} de_{ii}^A = \frac{1}{n} \left(1 - (1 - 2e_{ii}^A)^{\frac{n}{2}} \right), \quad (1)$$

where: n is strain measure coefficient; e_{ii}^A is Almansi finite strain component; and $i = 1, 2, 3$. It gives $n = -2, -1, 0, 1, 2$ respectively to Green, Cauchy, Hencky, Swainger and Almansi measures.

In this research, we investigated the problem of elastoplastic deformation in a transversely isotropic rotating disc having variable density with shaft subjected to temperature gradient by using transition theory of Seth and generalized strain measure theory. Disc density ρ is assumed to vary across the radius as:

$$\rho = \rho_0 \left(\frac{r}{b} \right)^{-m}, \quad (2)$$

where: m is a parameter; and ρ_0 is a constant at $r = b$. Results are presented numerically and graphically.

MATHEMATICAL MODEL AND GOVERNING EQUATION

Consider a homogeneous disc mounted on a rigid shaft of transversely isotropic/isotropic material with density gradient due to Eq.(2) having central bore of inner radius a and outer radius b . As shown in Fig. 1, the disc rotates gradually increasing at angular speed ω around an axis

perpendicular to its plane and passes through the centre. It is assumed that the thickness of the disc is constant and sufficiently small to be effective in a state of plane stress ($\sigma_{zz} = 0$), and the temperature φ_0 is applied to the central bore of the internal surface of the disc.

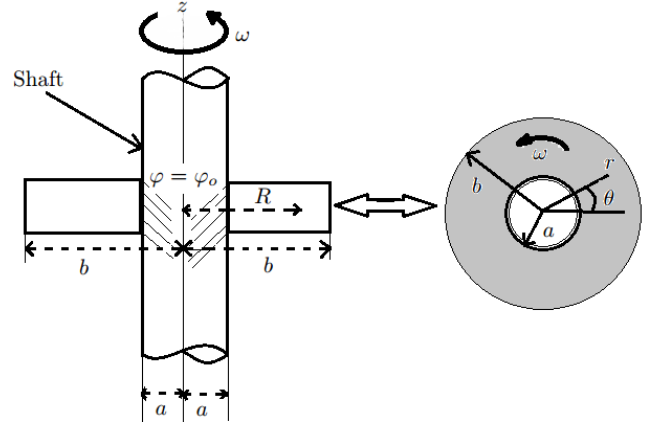


Figure 1. Rotating disc with shaft subjected to temperature gradient.

Boundary conditions

It is assumed that the disc's internal surface is fixed to a shaft and the outer surface is free from mechanical load. So, the problem's boundary conditions are set by:

$$\begin{aligned} r = a, \quad u = 0 \\ r = b, \quad \sigma_{rr} = 0, \end{aligned} \quad (3)$$

where: σ_{rr} and u are stress and displacement along the radial direction, respectively.

Displacement coordinates and strain measures

Since the shaft is strained symmetrically we can take the components of displacement in cylindrical coordinates as: $u = (1 - \eta)r$, $v = 0$, $w = dz$; η is a function of $r = \sqrt{x^2 + y^2}$ only; d is a constant which is the allowance for uniform longitudinal extension.

For finite deformation, the Almansi strain measures are:

$$\begin{aligned} e_{rr}^A &= \frac{\partial u}{\partial r} - \frac{1}{2} \left[\left(\frac{\partial u}{\partial r} \right)^2 + \left(\frac{\partial v}{\partial r} \right)^2 + \left(\frac{\partial w}{\partial r} \right)^2 - v^2 \right] = \frac{1}{2} [1 - (\beta + r\beta')^2] \\ e_{\theta\theta}^A &= \frac{1}{r} \frac{\partial v}{\partial \theta} + \frac{u}{r} - \frac{1}{2r^2} \left[\left(\frac{\partial u}{\partial \theta} \right)^2 + r^2 \left(\frac{\partial v}{\partial \theta} \right)^2 + \left(\frac{\partial w}{\partial \theta} \right)^2 \right] - \\ &\quad - \frac{1}{2r^2} \left[-vr^2 \frac{\partial u}{\partial \theta} + u \frac{\partial v}{\partial \theta} - v \frac{\partial u}{\partial \theta} + ur^2 \frac{\partial v}{\partial \theta} + u^2 + r^2 v^2 \right] = \\ &= \frac{1}{2} [1 - \beta^2] \\ e_{zz}^A &= \frac{\partial w}{\partial z} - \frac{1}{2} \left[\left(\frac{\partial u}{\partial z} \right)^2 + r \left(\frac{\partial v}{\partial z} \right)^2 + \left(\frac{\partial w}{\partial z} \right)^2 \right] = \frac{1}{2} [1 - (1 - d)^2], \\ e_{r\theta}^A &= e_{\theta z}^A = e_{zr}^A = 0, \end{aligned} \quad (4)$$

where: u, v, w are the physical components of displacement u_i and $e_{rr}^A, e_{\theta\theta}^A, e_{zz}^A, e_{r\theta}^A, e_{\theta z}^A, e_{zr}^A$ are the components of strain tensor e_{ij}^A ; the superscript 'A' is Almansi and $\eta' = d\eta/dr$.

Using Eqs.(4) into Eq.(1), the generalized components of strain are given by:

$$\begin{aligned} e_{rr} &= \frac{[1-(\eta+\eta'r)^n]}{n}, \quad e_{\theta\theta} = \frac{[1-\eta^n]}{n}, \\ e_{zz} &= \frac{[-(1-d)^n+1]}{n}, \quad e_{r\theta}=0=e_{\theta z}=e_{zr}. \end{aligned} \quad (5)$$

Stress-strain relation for transversely isotropic material

Thermoelastic constitutive equations are given by [17]:

$$\begin{aligned} e_{rr} &= \frac{\gamma}{\gamma^2 - \alpha^2} \left[\sigma_{rr} - \frac{\alpha}{\gamma} \sigma_{\theta\theta} \right] + \beta_2 \varphi \left[\frac{\alpha}{\gamma^2 - \alpha^2} \cdot \frac{C_{13}}{C_{33}} - \frac{\gamma}{\gamma^2 - \alpha^2} \cdot \frac{C_{13}}{C_{33}} - \frac{\alpha}{\gamma^2 - \alpha^2} \right] + \frac{\gamma}{\gamma^2 - \alpha^2} \cdot \beta_1 \varphi, \\ e_{\theta\theta} &= \frac{\gamma}{\gamma^2 - \alpha^2} \left[\sigma_{\theta\theta} - \frac{\alpha}{\gamma} \sigma_{rr} \right] + \beta_2 \varphi \left[\frac{\alpha}{\gamma^2 - \alpha^2} \cdot \frac{C_{13}}{C_{33}} - \frac{\gamma}{\gamma^2 - \alpha^2} \cdot \frac{C_{13}}{C_{33}} + \frac{\gamma}{\gamma^2 - \alpha^2} \right] + \frac{-\alpha}{\gamma^2 - \alpha^2} \cdot \beta_1 \varphi, \\ e_{zz} &= \frac{\beta_2 \varphi}{C_{33}} - \frac{C_{13}}{C_{33}} (e_{rr} + e_{\theta\theta}), \end{aligned} \quad (7)$$

where: $\gamma = C_{11} - \frac{C_{13}^2}{C_{33}}$ and $\alpha = \frac{C_{11}C_{33} - 2C_{66}C_{33} - C_{13}^2}{C_{33}} = \gamma - 2C_{66}$.

Let $\frac{1}{E} = \frac{\gamma}{\gamma^2 - \alpha^2}$ and $\nu = \frac{\alpha}{\gamma}$. Then Eq.(7) becomes

$$e_{rr} = \frac{1}{E} [\sigma_{rr} - \nu \sigma_{\theta\theta}] + \frac{\beta_2 \varphi}{E} \left[\nu \left(\frac{C_{13}}{C_{33}} - 1 \right) - \frac{C_{13}}{C_{33}} \right] + \frac{\beta_1 \varphi}{E}, \quad (8)$$

$$e_{\theta\theta} = \frac{1}{E} [\sigma_{\theta\theta} - \nu \sigma_{rr}] + \frac{\beta_2 \varphi}{E} \left[\left(1 - \frac{C_{13}}{C_{33}} \right) + \nu \frac{C_{13}}{C_{33}} \right] - \frac{\beta_1 \varphi \nu}{E}, \quad (9)$$

Using Eqs.(5) and (6), the stresses are obtained as

$$\begin{aligned} \sigma_{rr} &= C_{11} \frac{[1-(\eta+r\eta')^n]}{n} + (C_{11} - 2C_{66}) \frac{[1-\eta^n]}{n} + C_{13}e_{zz} - \beta_1\varphi, \\ \sigma_{\theta\theta} &= (C_{11} - 2C_{66}) \frac{[1-(\eta+r\eta')^n]}{n} + C_{11} \frac{[1-\eta^n]}{n} + C_{13}e_{zz} - \beta_2\varphi, \\ \sigma_{r\theta} &= 0 = \sigma_{\theta z} = \sigma_{zr} = \sigma_{zz}. \end{aligned} \quad (10)$$

$$\begin{aligned} C_{11}n p \eta^{n+1} (1+p)^{n-1} \frac{dp}{d\eta} &= -C_{11}n p \eta^n (1+p)^n - (C_{11} - 2C_{66})n p \eta^n + [1-\eta^n (1+p)^n] 2C_{66} - \\ &\quad - (1-\eta^n) 2C_{66} - n\beta_1 \bar{\varphi}_0 + (\beta_2 - \beta_1)n \bar{\varphi}_0 \ln\left(\frac{r}{b}\right) + n\rho_0 \left(\frac{r}{b}\right)^{-m} \omega^2 r^2, \end{aligned} \quad (13)$$

where: $r\eta' = p\eta$.

In Eq.(16) the transitional points of η are $p \rightarrow -1$ and $p \rightarrow \pm\infty$.

ANALYTICAL SOLUTION OF THE PROBLEM

The asymptotic solution leads from elastic to plastic state at the transition point $p \rightarrow \pm\infty$ via the principal stress (see

[7, 9-12]). We define the transition function ψ to find the plastic stress at the transition point as,

$$\psi = 2(C_{11} - C_{66}) + nC_{13}e_{zz} - n\sigma_{rr} - n\beta_1\varphi = \eta^n [C_{11} - 2C_{66} + C_{11}(1+p)^n]. \quad (14)$$

Then,

$$\frac{d}{dr} (\ln \psi) = \frac{m\eta^n p (C_{11} - 2C_{66} + C_{11}(1+p)^n) + nC_{11}p(1+p)^{n-1} \eta^{n+1} \frac{dp}{d\eta}}{r\psi}. \quad (15)$$

$$\begin{aligned} \sigma_{rr} &= C_{11}e_{rr} + (C_{11} - 2C_{66})e_{\theta\theta} + C_{13}e_{zz} - \beta_1\varphi, \\ \sigma_{\theta\theta} &= (C_{11} - 2C_{66})e_{rr} + C_{11}e_{\theta\theta} + C_{13}e_{zz} - \beta_2\varphi, \\ \sigma_{rz} &= 0 = \sigma_{r\theta} = \sigma_{\theta z} = \sigma_{zz}, \end{aligned} \quad (6)$$

where: $\beta_1 = \alpha_1 C_{11} + 2\alpha_2 C_{12}$; $\beta_2 = \alpha_1 C_{12} + \alpha_2 (C_{22} + C_{33})$; α_1 is the coefficient of linear thermal expansion across the axis of symmetry; α_2 is the corresponding quantity orthogonal to axis of symmetry; C_{ij} are elastic material parameters (constants); and φ is the temperature change.

From Eq.(6) and $\sigma_{zz} = 0$, strain components are obtained in terms of stress as:

The temperature field satisfying Fourier heat equation $\nabla^2 \varphi = \frac{1}{r} \frac{d}{dr} \left(r \frac{d\varphi}{dr} \right) = 0$ and $\varphi = \varphi_0$ at $r = a$, $\varphi = 0$ at $r = b$,

where φ_0 is a constant, from Seth: solving the heat equation using the given condition, we get:

$$\varphi = \bar{\varphi}_0 \ln(r/b), \quad (11)$$

where: $\bar{\varphi}_0 = \frac{\varphi_0}{\ln(a/b)}$.

All equilibrium stress equations are satisfied except:

$$\frac{d(\sigma_{rr})}{dr} + \frac{\sigma_{rr} - \sigma_{\theta\theta}}{r} + \rho \omega^2 r = 0, \quad (12)$$

where: ρ is the density of the material.

Substituting Eqs.(10) and (11) into Eq.(12), we obtain a nonlinear differential equation in η as:

From Eq.(13) substitute the value of $dp/d\eta$ in Eq.(15), we get

$$\frac{d}{dr}(\ln \psi) = \frac{2C_{66}(1-(1+p)^n) - \frac{n}{\eta^n} \left(\beta_1 \bar{\varphi}_0 + (\beta_1 - \beta_2) \bar{\varphi}_0 \ln\left(\frac{r}{b}\right) - \rho_0 \omega^2 r^2 \left(\frac{r}{b}\right)^{-m} \right)}{r [C_{11} - 2C_{66} + C_{11}(1+p)^n]}. \quad (16)$$

By taking asymptotic value of Eq.(16) as $p \rightarrow \pm\infty$, we get

$$\frac{d(\ln \psi)}{dr} = \frac{-2C_{66}}{rC_{11}}. \quad (17)$$

Let $C_1 = 2C_{66}/C_{11}$. Then from Eq.(17)

$$\psi = Ar^{-C_1}, \quad (18)$$

where: A is an integration constant.

Using Eq.(18) in Eq.(14), we get

$$\sigma_{rr} = \frac{2(C_{11} - C_{66})}{n} - \beta_1 \bar{\varphi}_0 \ln(r/b) - \frac{Ar^{-C_1}}{n}. \quad (19)$$

Let $\beta_0 = \beta_1 \bar{\varphi}_0$ and $C_3 = 2(C_{11} - C_{66})/n$. Thus, Eq.(19) becomes

$$\sigma_{rr} = C_3 - \beta_0 \ln(r/b) - \frac{Ar^{-C_1}}{n}. \quad (20)$$

Substituting Eq.(20) in Eq.(12), we get

$$\sigma_{\theta\theta} = C_3 - \beta_0 \left(1 + \ln\left(\frac{r}{b}\right) \right) - \frac{A}{n} (1 - C_1) r^{-C_1} + \rho_0 \left(\frac{r}{b}\right)^{-m} \omega^2 r^2. \quad (21)$$

To determine the displacement of the rotating disc, we use Eqs.(5), (9), (20) and (21), so we get:

$$u = r - r \sqrt{1 - \frac{2}{E} \left[C_3(1-\nu) - \frac{A}{n} r^{-C_1} ((1-\nu) - C_1) - \beta_0 \left(\ln\left(\frac{r}{b}\right) + 1 \right) + \rho_0 \left(\frac{r}{b}\right)^{-m} \omega^2 r^2 + g \right]}, \quad (22)$$

$$\text{where: } g = \beta_2 \bar{\varphi}_0 \ln(r/b) \left(1 - \frac{C_{13}}{C_{33}} (1-\nu) \right).$$

To compute the constants A and C_3 , we use the boundary conditions Eq.(3) in Eqs.(20) and (22). Thus,

$$C_3 = \frac{\beta_0 + \beta_0 \ln\left(\frac{a}{b}\right) - \rho_0 \left(\frac{a}{b}\right)^{-m} a^2 \omega^2 - \beta_2 \bar{\varphi}_0 \ln\left(\frac{a}{b}\right) \left[1 - \frac{C_{13}}{C_{33}} (1-\nu) \right]}{(1-\nu) - \left(\frac{b}{a}\right)^{C_1} ((1-\nu) - C_1)}, \quad (23)$$

$$A = nC_3 b^{C_1}. \quad (24)$$

Using the value of A and C_3 in Eq.(20), we get

$$\sigma_{rr} = \frac{\left(\left(\frac{b}{r}\right)^{C_1} - 1 \right) \left[\rho_0 a^2 \omega^2 \left(\frac{a}{b}\right)^{-m} - \beta_2 \bar{\varphi}_0 \ln\left(\frac{a}{b}\right) \left(\frac{C_{13}}{C_{33}} (1-\nu) - 1 \right) - \beta_0 \left(1 + \ln\left(\frac{a}{b}\right) \right) \right] + (-\beta_0 \ln(r/b)) \left[C_1 \left(\frac{b}{a}\right)^{C_1} - (1-\nu) \left(\left(\frac{b}{a}\right)^{C_1} - 1 \right) \right]}{C_1 \left(\frac{b}{a}\right)^{C_1} - (1-\nu) \left(\left(\frac{b}{a}\right)^{C_1} - 1 \right)}. \quad (25)$$

Using Eq.(25) in Eq.(12), we get

$$\sigma_{\theta\theta} = \frac{\left(\left(\frac{b}{r}\right)^{C_1} - C_1 \left(\frac{b}{r}\right)^{C_1} - 1 \right) \left[\rho_0 a^2 \omega^2 \left(\frac{a}{b}\right)^{-m} - \beta_2 \bar{\varphi}_0 \ln\left(\frac{a}{b}\right) \left(\frac{C_{13}}{C_{33}} (1-\nu) - 1 \right) - \beta_0 \left(1 + \ln\left(\frac{a}{b}\right) \right) \right] + \left(-\beta_0 - \beta_0 \ln(r/b) + \rho_0 r^2 \omega^2 \left(\frac{r}{b}\right)^{-m} \right) \left[C_1 \left(\frac{b}{a}\right)^{C_1} - (1-\nu) \left(\left(\frac{b}{a}\right)^{C_1} - 1 \right) \right]}{C_1 \left(\frac{b}{a}\right)^{C_1} - (1-\nu) \left(\left(\frac{b}{a}\right)^{C_1} - 1 \right)}. \quad (26)$$

From Eqs.(25) and (26), we get

$$\sigma_{rr} - \sigma_{\theta\theta} = \frac{C_1 \left(\frac{b}{r}\right)^{C_1} \left[\rho_0 a^2 \omega^2 \left(\frac{a}{b}\right)^{-m} - \beta_2 \bar{\varphi}_0 \ln\left(\frac{a}{b}\right) \left(\frac{C_{13}}{C_{33}} (1-\nu) - 1 \right) - \beta_0 \left(1 + \ln\left(\frac{a}{b}\right) \right) \right] + \left(\beta_0 - \rho_0 r^2 \omega^2 \left(\frac{r}{b}\right)^{-m} \right) \left[C_1 \left(\frac{b}{a}\right)^{C_1} - (1-\nu) \left(\left(\frac{b}{a}\right)^{C_1} - 1 \right) \right]}{C_1 \left(\frac{b}{a}\right)^{C_1} - (1-\nu) \left(\left(\frac{b}{a}\right)^{C_1} - 1 \right)}. \quad (27)$$

Using Eqs.(23) and (24) in Eq.(22), we get

$$u = r - r \sqrt{1 - \frac{2}{E} \left[\frac{\rho_0 \omega^2}{b^{-m}} (r^{2-m} - a^{2-m}) + \ln \left(\frac{a}{r} \right) \left(\beta_0 - \beta_2 \bar{\varphi}_0 \left(1 - \frac{C_{13}}{C_{33}} (1-\nu) \right) \right) \right]}. \quad (28)$$

Initial yielding

For the discs made of transversely isotropic materials (magnesium and beryl), it has been found that the value of $|\sigma_{\theta\theta}|$ is maximum at $r = b$, which means yielding will occur on the outer surface of the discs. Thus,

$$|\sigma_{\theta\theta}|_{r=b} = \frac{(-C_1 - 1) \left[\rho_0 a^2 \omega^2 \left(\frac{a}{b} \right)^{-m} - \beta_2 \bar{\varphi}_0 \ln \left(\frac{a}{b} \right) \left(\frac{C_{13}}{C_{33}} (1-\nu) - 1 \right) - \beta_0 \left(1 + \ln \left(\frac{a}{b} \right) \right) \right] + (-\beta_0 + \rho_0 b^2 \omega^2) \left[C_1 \left(\frac{b}{a} \right)^{C_1} - (1-\nu) \left(\left(\frac{b}{a} \right)^{C_1} - 1 \right) \right]}{C_1 \left(\frac{b}{a} \right)^{C_1} - (1-\nu) \left(\left(\frac{b}{a} \right)^{C_1} - 1 \right)} \equiv Y. \quad (29)$$

For the discs made of isotropic material (steel), it has been found that the value of $|\sigma_{\theta\theta}|$ is maximum at $r = b$, which means yielding occurs at the outer surface of the discs depending on the value of m . Thus,

$$|\sigma_{\theta\theta}|_{r=b} = \frac{(-C_1 - 1) \left[\rho_0 a^2 \omega^2 \left(\frac{a}{b} \right)^{-m} - \beta_2 \bar{\varphi}_0 \ln \left(\frac{a}{b} \right) \left(\frac{C_{13}}{C_{33}} (1-\nu) - 1 \right) - \beta_0 \left(1 + \ln \left(\frac{a}{b} \right) \right) \right] + (-\beta_0 + \rho_0 b^2 \omega^2) \left[C_1 \left(\frac{b}{a} \right)^{C_1} - (1-\nu) \left(\left(\frac{b}{a} \right)^{C_1} - 1 \right) \right]}{C_1 \left(\frac{b}{a} \right)^{C_1} - (1-\nu) \left(\left(\frac{b}{a} \right)^{C_1} - 1 \right)} \equiv Y, \quad (30)$$

$m = 1$

$$|\sigma_{rr}|_{r=a} = \frac{\left(\left(\frac{b}{a} \right)^{C_1} - 1 \right) \left[\rho_0 a^2 \omega^2 \left(\frac{a}{b} \right)^{-m} - \beta_2 \bar{\varphi}_0 \ln \left(\frac{a}{b} \right) \left(\frac{C_{13}}{C_{33}} (1-\nu) - 1 \right) - \beta_0 \left(1 + \ln \left(\frac{a}{b} \right) \right) \right] + (-\beta_0 \ln(a/b)) \left[C_1 \left(\frac{b}{a} \right)^{C_1} - (1-\nu) \left(\left(\frac{b}{a} \right)^{C_1} - 1 \right) \right]}{C_1 \left(\frac{b}{a} \right)^{C_1} - (1-\nu) \left(\left(\frac{b}{a} \right)^{C_1} - 1 \right)} \equiv Y, \quad (31)$$

where: Y is the yielding stress.

Elastoplastic stresses and displacement

The non-dimensional quantities are introduced as

$$R = \frac{r}{b}, \quad R_0 = \frac{a}{b}, \quad \sigma_r = \frac{\sigma_{rr}}{Y}, \quad \sigma_\theta = \frac{\sigma_{\theta\theta}}{Y}, \quad \bar{u} = \frac{u}{b}, \quad \beta_3 = \frac{\beta_0}{Y},$$

$$\Omega^2 = \frac{\rho_0 \omega^2 b^2}{Y}, \quad H = \frac{Y}{E}.$$

Elastoplastic stresses and displacement from Eqs.(25), (26) and (28) in non-dimensional form become:

$$\sigma_r = \frac{\left(R^{-C_1} - 1 \right) \left[\Omega^2 R_0^{2-m} - \beta_3 \left(\frac{\beta_2}{\beta_1} \ln R_0 \left(\frac{C_{13}}{C_{33}} (1-\nu) - 1 \right) + (1 + \ln R_0) \right) \right] + (-\beta_3 \ln R) \left[C_1 R_0^{-C_1} - (1-\nu) \left(R_0^{-C_1} - 1 \right) \right]}{C_1 R_0^{-C_1} - (1-\nu) \left(R_0^{-C_1} - 1 \right)}, \quad (32)$$

$$\sigma_\theta = \frac{\left(R^{-C_1} - C_1 R^{-C_1} - 1 \right) \left[\Omega^2 R_0^{2-m} - \beta_3 \left(\frac{\beta_2}{\beta_1} \ln R_0 \left(\frac{C_{13}}{C_{33}} (1-\nu) - 1 \right) + (1 + \ln R_0) \right) \right] - \left(\beta_3 (1 + \ln R) - \Omega^2 R^{2-m} \right) \left[C_1 R_0^{-C_1} - (1-\nu) \left(R_0^{-C_1} - 1 \right) \right]}{C_1 R_0^{-C_1} - (1-\nu) \left(R_0^{-C_1} - 1 \right)}, \quad (33)$$

$$\bar{u} = R - R \sqrt{1 - 2H \left[\Omega^2 \left(R^{2-m} - R_0^{2-m} \right) + \beta_3 \ln \left(\frac{R_0}{R} \right) \left(1 - \frac{\beta_2}{\beta_1} \left(1 - \frac{C_{13}}{C_{33}} (1-\nu) \right) \right) \right]}. \quad (34)$$

NUMERICAL ILLUSTRATION AND DISCUSSION

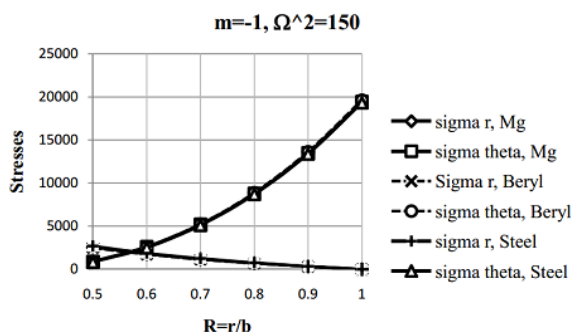
Elastic stiffness constants C_{ij} are given in Table 1 for transversely isotropic materials (magnesium and beryl) and isotropic material (steel). Based on the above analysis, the following values are taken into account for calculating elastic-plastic stresses and displacement: $m = -1, 0, 1$; $\beta_3 =$

$0, 0.5, 0.75$; $\beta_2/\beta_1 = 1$ and $\Omega^2 = 150, 250, 350$. Curves are drawn for transversely isotropic/isotropic rotating disc between stresses and displacement along the radii ratio R . In Figs. 2, 3 and 4 we use σ_r instead of σ_r , σ_θ instead of σ_θ , displacement instead of \bar{u} and Ω^2 instead of Ω^2 .

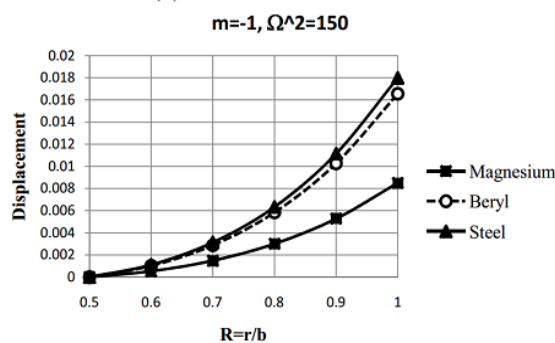
Table 1. Elastic stiffness constants C_{ij} used in units of 10^{10} N/m².

Materials	C_{11}	C_{12}	C_{13}	C_{33}	C_{44}
Transv. isotropic ($C_1 = 0.561$, Mg)	5.97	2.62	2.17	6.17	1.64
Transv. isotropic ($C_1 = 0.643$, Be)	2.746	0.980	0.674	4.690	0.883
Isotropic ($C_1 = 0.563$, steel)	2.908	1.27	1.27	2.908	0.819

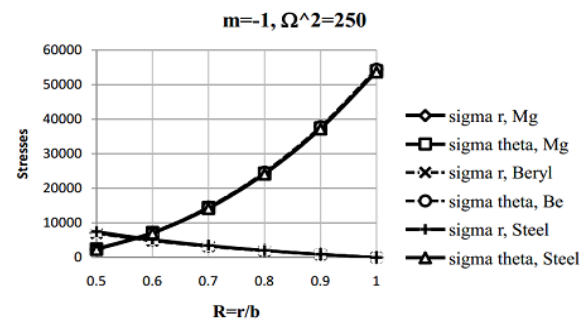
It is observed from Fig. 2 that as the density decreases from external to internal rotating disc made of transversely isotropic materials, the isotropic material yields at the external surface with the increase of angular speed and temperature. Furthermore, as the density decreases and the rotation speed increases, the circumferential stress values of the three materials: magnesium, beryl, and steel, are increased. The circumferential stress values of the transversely isotropic materials are higher than the isotropic material. The radial stresses of the three materials Mg, Be, and steel are very small as compared to the tangential stresses. The radial stress of isotropic material (steel) is greater than transversely isotropic materials (Mg and Be). The displacement of the rotating disc made of an isotropic material is higher than the displacement of the disc made of transversely isotropic materials, especially the displacement of the rotating disc of Mg is much lower than Be. As the angular speed increases, the displacement of the rotating disc of both materials increases, but at a higher angular speed the displacement of steel and Be decrease after certain values of the radii ratio, so that the displacement of Mg is higher than for Be and steel.



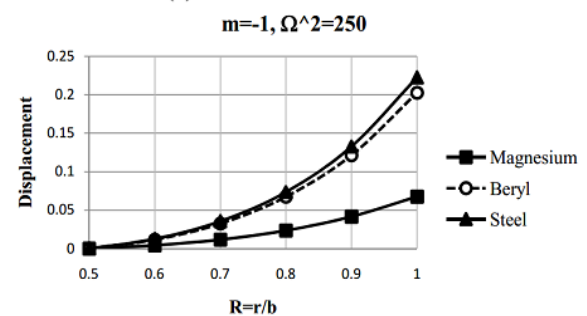
(a) Stresses Vs Radii ratio



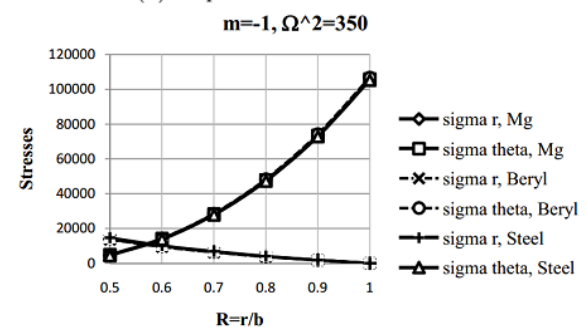
(b) Displacement Vs Radii ratio



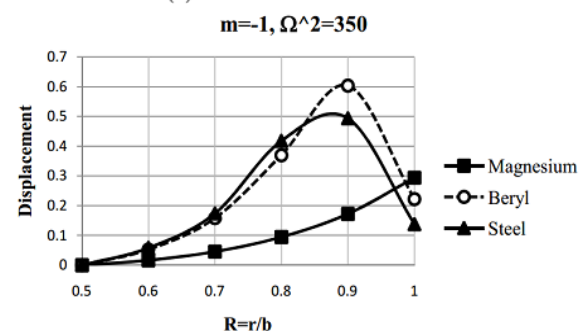
(c) Stresses Vs Radii ratio



(d) Displacement Vs Radii ratio



(e) Stresses Vs Radii ratio

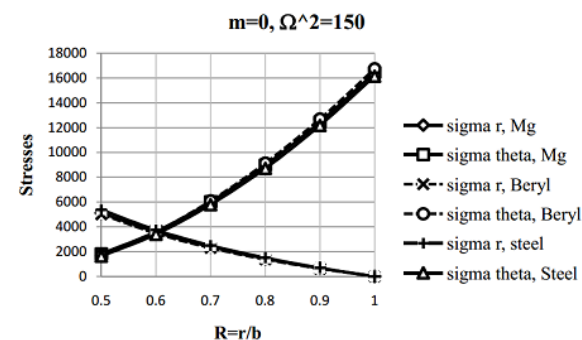


(f) Displacement Vs Radii ratio

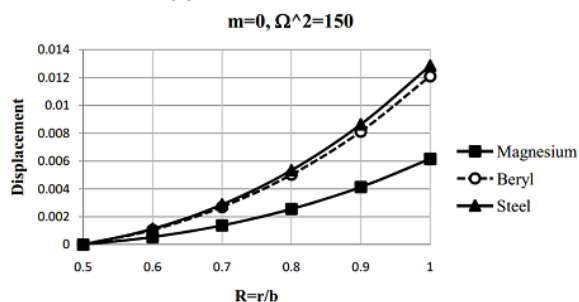
Figure 2. Distribution of elastic-plastic stresses and displacement in the disc having the parameter $m = -1$ under different rotating speed and temperature.

In Fig. 3, the curves are drawn between stresses and the displacement along the radii ratio R for parameters $m = 0$; $\beta_3 = 0, 0.5, 0.75$ and $\Omega^2 = 150, 250, 350$. It is seen that as the density of the disc is constant, the transversely isotropic/isotropic disc yields on the external surface at a higher

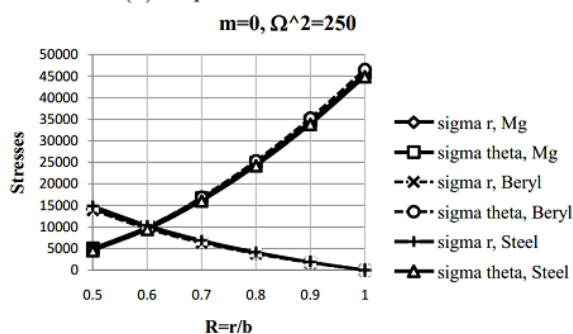
angular speed and temperature. In Fig. 3 the radial stresses are increased as compared to the radial stress in Fig. 2. The displacement of isotropic rotating disc is higher than the displacement of transversely isotropic rotating disc. As the angular speed increases, the displacement of rotating disc made of both materials increases, but at higher angular speed and near to external surface, the displacement of steel decreases and the displacement of beryl is constant.



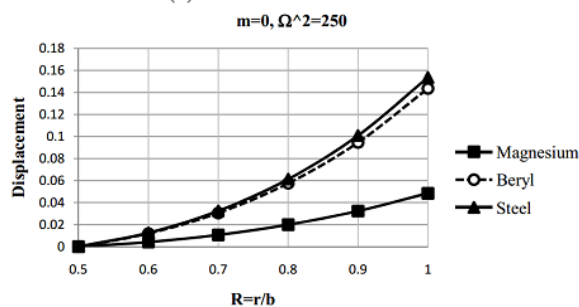
(a) Stresses Vs Radii ratio



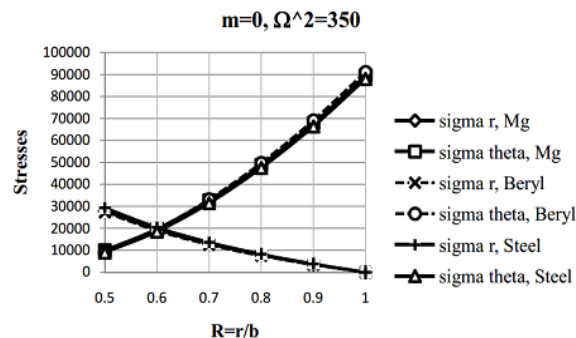
(b) Displacement Vs Radii ratio



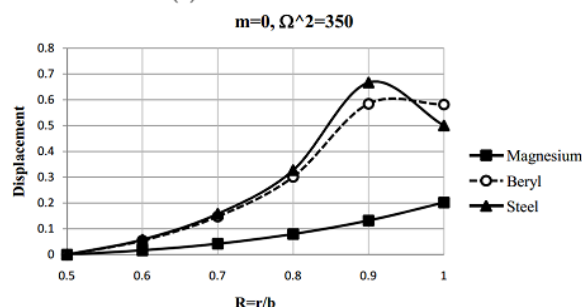
(c) Stresses Vs Radii ratio



(d) Displacement Vs Radii ratio



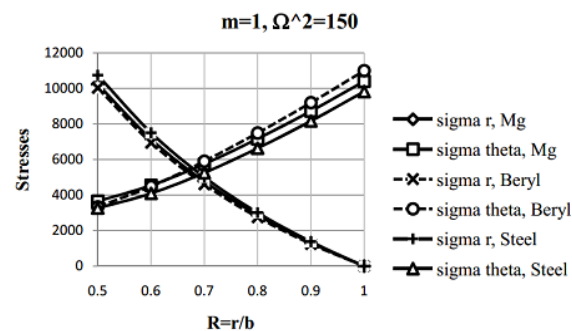
(e) Stresses Vs Radii ratio



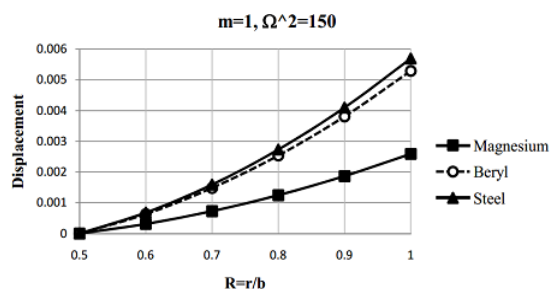
(f) Displacement Vs Radii ratio

Figure 3. Distribution of elastic-plastic stresses and displacement in the disc having the parameter $m = 0$ under different rotating speed and temperature.

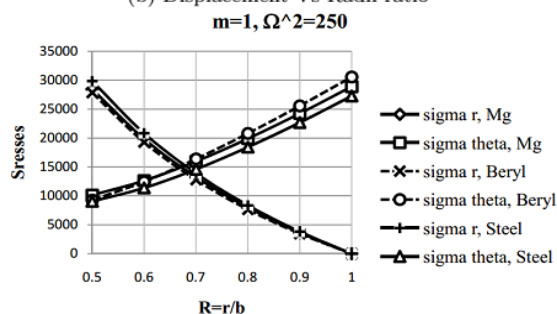
It is observed from Fig. 4 that as the density increases from external to internal, transversely isotropic rotating disc yields at the external surface, but the isotropic rotating disc yields at the internal surface at higher angular speed and temperature. Further, as the rotational speed of the disc increases, the circumferential stresses increase, and radial stresses decrease. Circumferential stress values of the disc made of beryl are higher than for magnesium and the radial stress value of the disc of steel is greater than the case with magnesium and beryl. The displacement of the rotating disc made of an isotropic material is higher than in the case of disc made of transversely isotropic materials. As angular speed increases the displacement of the rotating disc made of both materials increases and the displacement of rotating disc made of magnesium material is smaller as compared to beryl and steel. The displacement of rotating disc made of materials magnesium, beryl, and steel increases from the internal to the external surface.



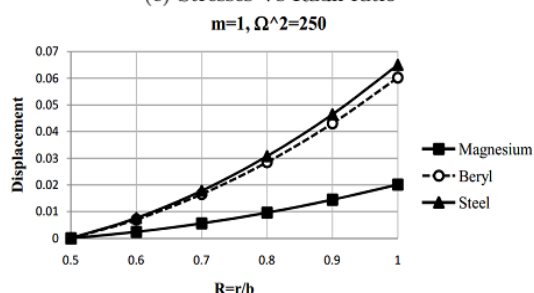
(a) Stresses Vs Radii ratio



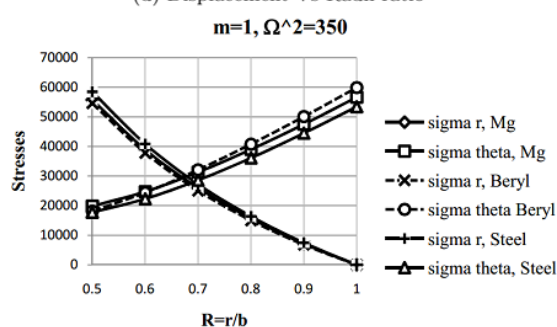
(b) Displacement Vs Radii ratio



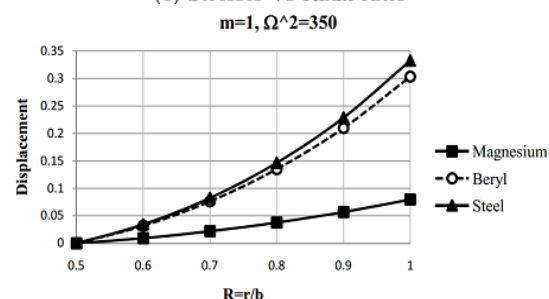
(c) Stresses Vs Radii ratio



(d) Displacement Vs Radii ratio



(e) Stresses Vs Radii ratio



(f) Displacement Vs Radii ratio

Figure 4. Distribution of elastic-plastic stresses and displacement in the disc with parameter $m = 1$ vs. rotating speed and temperature.

CONCLUSION

It is concluded that transversely isotropic/isotropic rotating disc yields at the external surface with the increase of angular speed and temperature as the disc density decreases or is constant from external to internal surface. Further, as the disc density decreases or is constant from external to internal surface, the displacement of steel and beryl near to the external surface decreases at high angular speed and temperature. It is also observed that as the density increases from external to internal surface, the rotating disc of transversely isotropic materials yields at the external surface, but the isotropic material yields at the internal surface with the increase of angular speed and temperature. The radial stress of rotating disc made of an isotropic material is greater than the radial stress of transversely isotropic materials and the circumferential stresses of transversely isotropic materials are greater than in isotropic material. The displacement of isotropic rotating disc is higher than the displacement of the transversely isotropic rotating disc. The displacement of transversely isotropic/isotropic rotating disc increases with the increase of angular speed.

REFERENCES

1. Boresi, A.P., Schmidt, R.J., Advanced Mechanics of Materials, Sixth Ed., John Wiley & Sons, Inc., New York, 2003.
2. Chakrabarty, J., Applied Plasticity, Springer-Verlag, New York/Berlin/Heidelberg, 2000.
3. Fung, Y.C., Foundations of Solid Mechanics, Englewood Cliffs, N.J., Prentice-Hall, 1965.
4. Gupta, V.K., Singh, S.B., Chandrawat, H.N., Ray, S. (2004), *Steady state creep and materials parameters in a rotating disc of Al-SiC_p*, European J Mechanics-A/Solids, 23(2): 335-344. doi: 10.1016/j.euromechsol.2003.11.005
5. Hetnarski, R.B., Ignaczak, J., Mathematical Theory of Elasticity, Taylor and Francis, New York, USA, 2004.
6. László, F. (1925), *Geschleuderte umdrehungskörper im Gebiet bleibender Deformation*, ZAMM, 5(4):281-293. doi: 10.1002/zamm.19250050402
7. Thakur, P. (2010), *Elastic-plastic transition stresses in a thin rotating disc with rigid inclusion by infinitesimal deformation under steady-state temperature*, Thermal Science, 14(1):209-219. doi: 10.2298/TSCI1001209P
8. Parkus, H., Thermo-Elasticity, Springer-Verlag Wien, New York, USA, 1976. doi: 10.1007/978-3-7091-8447-9
9. Seth, B.R. (1962), *Transition theory of elastic-plastic deformation, creep and relaxation*, Nature, 195: 896-897. doi: 10.1038/195896a0
10. Seth, B.R. (1966), *Generalized strain and transition concepts for elastic-plastic deformation-creep and relaxation*, Appl. Mech., 383-389. doi: 10.1007/978-3-662-29364-5_51
11. Seth, B.R. (1964), *On the problem of transition phenomenon, i(Asymptotic representation of transition phenomena in elastoplastic deformation and creep rupture)*, IASI, Inst. Politehnic, Biletinul, 10(1): 255-262.
12. Seth, B.R. (1966), *Measure-concept in mechanics*, Int. J Non-Linear Mech. 1(1):35-40. doi.org/10.1016/0020-7462(66)90016-3
13. Singh, S.B. (2008), *One parameter model for creep in a whisker reinforced anisotropic rotating disc of Al-SiC_w composite*, Europ. J Mech.-A/Solids, 27(4):680-690. doi: 10.1016/j.euromechsol.2007.11.004
14. Singh, S.B., Ray, S. (2003), *Creep analysis in an isotropic FGM rotating disc of Al-SiC composite*, J Mater. Proc. Techn. 143-144 : 616-622. doi: 10.1016/S0924-0136(03)00445-X

15. Singh, S.B., Ray, S. (2003), *Newly proposed yield criterion for residual stress and steady state creep in an anisotropic composite rotating disc*, J Mater. Proc. Techn. 143-144 : 623-628. doi: 10.1016/S0924-0136(03)00446-1
16. Singh, S.B., Ray, S. (2002), *Modeling the anisotropy and creep in orthotropic aluminum-silicon carbide composite rotating disc*, Mechanics of Mater. 34(6): 363-372.
17. Sokolnikoff, I.S., *Mathematical Theory of Elasticity*, Second Ed., McGraw-Hill Book Co., New York, 1956.

18. Timoshenko, S.P., Goodier, J.N., *Theory of Elasticity*, Third Ed., Mc Graw-Hill Book Co. New York, London, 1951.

© 2020 The Author. Structural Integrity and Life, Published by DIVK (The Society for Structural Integrity and Life 'Prof. Dr Stojan Sedmak') (<http://divk.inovacionicentar.rs/ivk/home.html>). This is an open access article distributed under the terms and conditions of the Creative Commons Attribution-NonCommercial-NoDerivatives 4.0 International License

ECF23, European Conference on Fracture 2022

June 27 – July 1, 2022. Funchal, Madeira, Portugal

Fracture Mechanics and Structural Integrity

Sponsored by ESIS – European Structural Integrity Society

Unfortunately, the Corona virus pandemic problem has evolved to a situation that makes the realization of ECF23, on its present schedule, not possible. New deadline for ESIS Support for Researchers: March 31st, 2022

Dear Colleagues,

On behalf of the European Structural Integrity Society (ESIS) we have the pleasure to extend a warm welcome to all researchers planning to attend the 23rd European Conference on Fracture – ECF23, scheduled from June 27-July 1, 2022, on the beautiful Madeira Island, Portugal.

A Summer School on 25-26 June 2022, will take place as part of the conference. The two days event is mainly aimed at PhD students, young researchers and engineers, but it is open to everybody.

The conference will be held on one of the most emblematic hotels in Funchal, authored by the genius of Oscar Niemeyer, the Casino Park Hotel. The huge offer of hotels in Funchal provides the necessary conditions for every sort of visitors, constituting an invaluable argument for the organisation of a large conference such as ECF.

ECF23 focus will be twofold, on dynamical aspects of Structural Integrity and the largely unobserved realm of Integrity loss under dynamical loads as well as the developments of the monitoring technical aspects and their pitfalls as dynamics particularities take precedence over the phenomena we have come to know so well.

Aim and Topics

The conference topics include but are not limited to:

Additive Manufacturing; Adhesives; Analytical, computational and physical models; Artificial Intelligence, Machine Learning and Digitalization in Fracture and Fatigue; Biomechanics; Ceramics; Composites; Computational Mechanics; Concrete & Rocks; Corrosion; Creep; Damage Mechanics; Durability; Environmentally Assisted Fracture; Experimental Mechanics; Failure Analysis and Case Studies; Fatigue; Fatigue Crack Growth; Fractography and Advanced metallography; Fracture and fatigue testing systems; Fracture and fatigue of additively manufactured materials or structures; Fracture and fatigue problems in regenerative energy systems (wind turbines, solar cells, fuel cells,...); Fracture under Mixed-Mode and Multiaxial Loading; Functional Graded Materials; Hydrogen embrittlement; Image analysis techniques Impact & Dynamics; Innovative Alloys; Joints and Coatings; Linear and Nonlinear Fracture Mechanics; Mesomechanics of Fracture; Micromechanisms of Fracture and Fatigue; Multi-physics and multi-scale modelling of cracking in heterogeneous materials; Nanomaterials; Non-destructive inspection; Polymers; Probabilistic Fracture Mechanics; Reliability and Life Extension of Components; Repair and retrofitting; modelling and practical applications; Smart Materials; Structural Integrity; Temperature Effects; Thin Films



Conference Chairmen

Pedro M. G. P. Moreira, Phone: +351 22 041 4902

Luís Reis, IST, Phone: +351 96 641 5585

Email : ecf23@ecf23.eu

Important deadlines

Abstract submission, please submit your work by email to ecf23@ecf23.eu by February 28, 2022

Abstract acceptance notification by March 05, 2022

Full paper submission (Procedia) by August 20, 2022

Authors are invited to submit a maximum of two one-page abstracts (in English). All abstracts will be peer-reviewed based on originality, technical quality and presentation. The abstract should be prepared according to the template, which can be downloaded from http://ecf23.eu/abstract_ECF23.docx and submitted by email to ecf23@ecf23.eu

When submitting an abstract for a particular symposium please indicate so in your email.

Publication in Elsevier Journal

Authors are encouraged to submit a full conference paper of 6-8 pages. Reviewed and accepted conference papers will be published in a dedicated issue in Elsevier's Procedia Structural Integrity and made available in open-access at <http://www.journals.elsevier.com/procedia-structural-integrity/> after the conference.

Your paper should be submitted by August 20, 2022, at the latest. Please note that your full manuscript should abide by the full paper template and follow the paper preparation guidelines, which are available at http://ecf23.eu/PROSTR_ECF23_Template.docm Full paper template: [Word template](#) , [Latex and Word template](#) (zip file)

Important: Getting your abstract accepted does not mean that you are registered for the conference. Remember to register and pay for the conference before April 15th, 2022, in order to get a discount on the participation fee. You can also book your accommodation and social arrangements through the conference registration.